J. Appl. Comput. Mech., 8(4) (2022) 1445-1455
DOI: 10.22055/jacm.2022.39487.3414

ISSN: 2383-4536
jacm.scu.ac.ir

Shahid Chamran University of Ahvaz

Journal of Applied and Computational Mechanics

Research Paper

Impact of the Narrowing System at Different Locations and Heights on the Performance of a Plane Solar Collector

Hamidou Benzenine[1,2], Said Abboudi[3]

[1] Department of Mechanical Engineering, Faculty of science and technology, University of BELHADJ Bouchaib, P.O. Box 284 RP, Ain Témouchent, 46000, Algeria
[2] Laboratory of Energetic and Applied Thermal (ETAP), Faculty of Technology, B.P 230, University of Tlemcen, 13000, Algeria, E-mail: b.hamidou@yahoo.fr
[3] ICB, UMR 6303 CNRS, Department COMM UTBM, University of Bourgogne Franche-Comte, 90010 Belfort Cedex, France, E-mail: said.abboudi@utbm.fr

Received December 18 2021; Revised May 07 2022; Accepted for publication June 06 2022.
Corresponding author: H. Benzenine (b.hamidou@yahoo.fr)

Abstract. This paper presents a numerical study of a solar air collector aiming at analyzing the influence of several geometrical parameters on the heat transfer mechanisms with minimum losses. The laminar airflow in the collector undergoes a sudden or gradual narrowing at the absorber in its path. The finite volume method is used to solve the conservative equations of the fluid flow in the system. The results for these two narrowing models, at different positions and heights, show an improvement in heat transfer and a reduction in friction, especially in the case of gradual narrowing. Both narrowing models reduce the recirculation zones and thus increase the fluid velocity (1.25 to 2.50 times the reference velocity), leading to a gain in pressure drop compared to the perpendicular shoulder case. This solution also increased system efficiency (22.41% to 50.12% for the inclined shoulder case, 21.83% to 48.86% for the perpendicular case, and 20.81% to 38.66% for the simple case).

Keywords: Forced convection, laminar, narrowing channel, solar collector, performance.

1. Introduction

The study of the efficiency and profitability of solar collectors has attracted the attention of many researchers. This system has been among the efficient means of using solar energy with low investment cost and preheats fresh air needed for various applications such as heating, drying, etc. [1-5]. Abene et al. [6] proposed an experimental study to improve the efficiency of a solar plate collector by considering several types of obstacles arranged in rows in the dynamic air duct of the collector. Ahmed-Zaïd et al. [7] introduced baffles in the fluid stream of the collector. The authors numerically confirmed the efficiency of this technique for drying some products such as yellow onion and herring. In the article by Gopi et al. [8], cylindrical fins placed at the absorber plate for different arrangements are used to improve the performance of the solar collector. The study revealed that the rate of heat transfer with a staggered arrangement of cylindrical fins is maximum compared to a linear arrangement.

Mzad et al. [9, 10] proposed a study related to double-glazed solar collectors and determined thermal parameters such as fluid temperature and panel efficiency in northwest Algeria. Inclination optimization was also performed through an empirical thermal model for an air-source solar collector tested in northeast Algeria. An experimental study was carried out by Ravi and Saini [11] on a double-pass collector with a flat and corrugated V-shaped absorber. This study revealed a 4.5 and 3.1 times increase in Nu number and friction factor respectively for V corrugated absorbers compared to a flat plate.

Ahmad and Tiwari [12] examined the theoretical aspects of inclination angle selection for flat plate solar collectors used in ten different stations worldwide. Their results show that an almost optimum amount of energy can be collected if the inclination angle is changed seasonally, four times a year. Furthermore, the average annual energy loss is about 15% when the angle is fixed than the optimal monthly inclination.

Yang et al. [13] compared the influence of five critical parameters (1) heat transfer resistance in the channel, (2) height of the thick air layer, (3) optical properties of the transparent cover, (4) emittance of the absorber plate and (5) thermal resistance of the backplate, on the thermal performance of a single-pass collector. Their results show that decreasing the heat transfer resistance in the channel played the most important role in improving thermal performance. Adjusting the thick air layer's height and improving the transparent cover's optical properties increasing the thermal resistance of the backplate, and decreasing the emittance of the absorber plate had the least impact.

Ravi and Saini [14] experimentally investigated the effect of roughness on the thermal-hydraulic performance of double-pass collectors with discrete, multi-V offset ribs. It was found that the roughness geometry used on each side of the plate improves the frictional losses and the heat dissipation rate. The recent studies on various absorber configurations and its effect on improving the thermal performance of flat plate solar collectors have been presented in the work of Elumalai and Ramalingam [15]. The

Published online: June 19 2022

authors also showed that increasing the roughness of the surface of the absorber also increases the pressure drop and the cost of pumping.

Two solar air collectors with different shapes, wavy-shaped and trapezoidal, were constructed and examined experimentally by Hüseyin Benli [16]. The researcher concluded that the ANN (Artificial Neural Network) method could be used to predict the thermal performance of solar air collectors as an accurate method in this system.

Many researchers have suggested that modifying the structure of absorber plates could improve the heat transfer of solar thermal converters. Several thermal enhancement techniques have been used, but most are associated with additional pressure drops (Chinmaya et al. [17]). In addition, few studies have focused on a system to accelerate fluid flow; this technique is in great demand for many applications such as solar drying, heating, ventilation, etc.

This study aims to improve the dynamic and thermal performances of a laminar flow in the airplane of a solar collector by introducing in the airflow channel, inserted on the absorber, a shoulder of perpendicular and inclined shape. This study examines the influence of the position of the shoulder and the effect of variations in its height on temperature variation, collector outlet velocity, friction, and drag force. They are also compared with conventional cases without a shoulder for a volume flow rate between 20 and 80 m^3/h.

2. Physical Model and Governing Equations

Figure 1 shows the geometrical configuration of the physical model. It is a planar solar collector studied by Labed et al. [5]. Table 1 lists the geometrical characteristics of the studied channel.

Several absorber designs with sudden (Fig. 2 (b), (c) and (d)) and gradual (Fig. 2(e), (f) and (g)) narrowing thickness were studied for three locations: e1 = L/4, e2 = L/2 and e3 = 3L/4. For each case, three heights, h1 = 5 mm, h2 = 10 mm and h3 = 15 mm were compared to the simple case in Fig. 2(a).

The motion of the fluid in the channel is governed by the continuity, momentum, and energy equations. The following assumptions were made to simplify the analysis:

- The fluid is Newtonian and incompressible.
- The flow is laminar, stationary, and two-dimensional.
- The thermo-physical properties of the fluid and the solid are constant.
- The heat flow applied to the top wall is uniform.
- The inlet velocity and temperature profiles are constant.

Based on the above assumptions, the system of the governing into the solar collector plan is given by:

Continuity:

$$\frac{\partial u}{\partial x}+\frac{\partial v}{\partial y}=0 \tag{1}$$

Momentum:

$$u\frac{\partial u}{\partial x}+v\frac{\partial u}{\partial y}=-\frac{1}{\rho}\frac{\partial p}{\partial x}+\nu\left[\frac{\partial^2 u}{\partial x^2}+\frac{\partial^2 u}{\partial y^2}\right] \tag{2}$$

$$u\frac{\partial v}{\partial x}+v\frac{\partial v}{\partial y}=-\frac{1}{\rho}\frac{\partial p}{\partial y}+\nu\left[\frac{\partial^2 v}{\partial x^2}+\frac{\partial^2 v}{\partial y^2}\right] \tag{3}$$

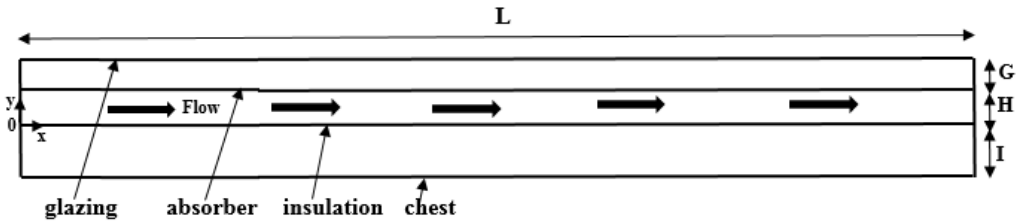

Fig. 1. Schematic description of the thermal collector.

Table 1. Characteristics of the reference geometry.

Channel length (L)	1.96	m
Channel width (l)	0.9	m
Thickness of the transparent glass cover	5	mm
Thickness of plate absorber galvanized steel painted in matt black	0.4	mm
Thickness of the galvanized steel backplate placed on the insulation	0.4	mm
Height between the transparent cover and the absorber plate (G)	20	mm
Height of dynamic air stream (H)	25	mm
Insulation thickness (polystyrene sheet) (I)	30	mm
Thickness of the wooden case behind the insulation	5	mm

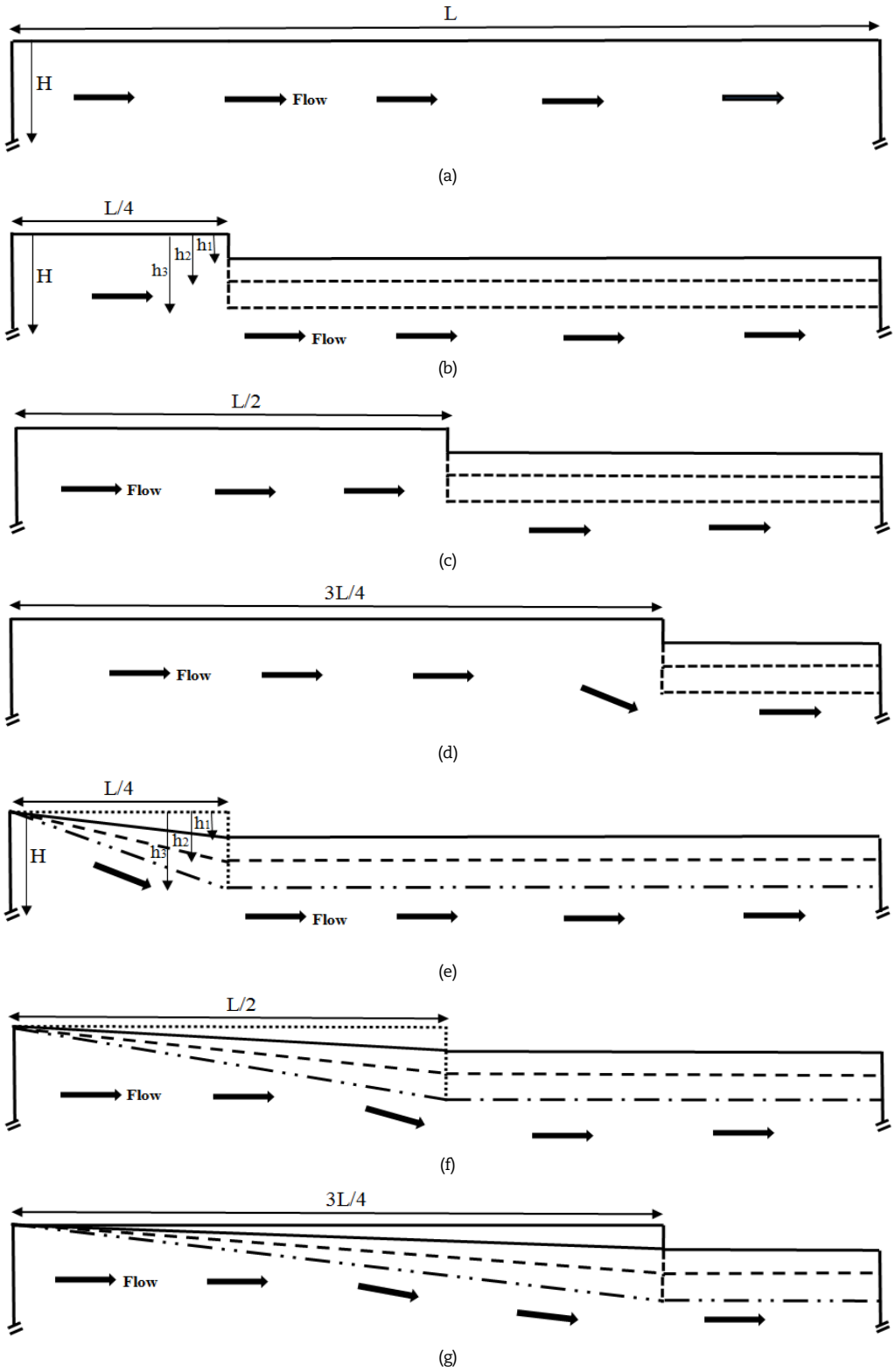

Fig. 2. Geometric configurations of the channel: (a) simple case (b), (c) and (d): sudden narrowing case; (e), (f) and (g): gradual narrowing case, at different locations and heights.

Energy:

$$\rho C_p\left(u\frac{\partial T}{\partial x}+v\frac{\partial T}{\partial y}\right)=k\left[\frac{\partial^2 T}{\partial x^2}+\frac{\partial^2 T}{\partial y^2}\right] \tag{4}$$

For each case, the exchange surface is greater than for the simple case $S_{simple}=L.l$.

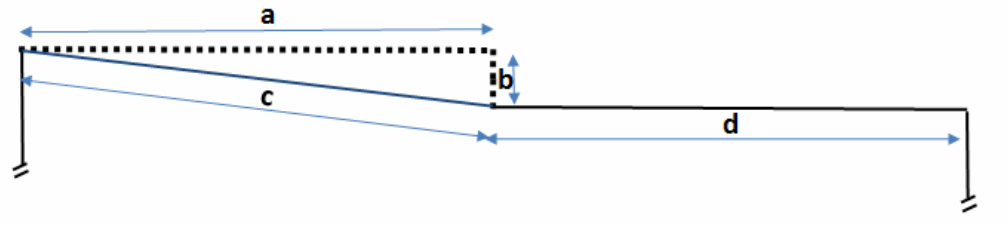

Fig. 3. Dimensions used for the calculation of the absorber's exchange surface.

- For a perpendicular shoulder:

$$S_{perp} = (a + b + d)l \tag{5}$$

- For inclined shoulder:

$$S_{inc} = \left(\sqrt{a^2 + b^2} + d\right)l \tag{6}$$

To correctly quantify the pressure losses, it is interesting to use the notion of drag coefficient:

$$C_d = \frac{2\Delta p}{\rho U_0^2}\left(\frac{A_f}{A_0}\right) \tag{7}$$

and the average friction coefficient:

$$\overline{C}_f = \frac{2\overline{\tau}_w}{\rho.U^2} \tag{8}$$

The calculation of the solar collector efficiency is defined as the ratio of the heat transferred by the fluid in the solar collector $\dot{Q}_c$ and the solar radiation absorbed by its surface $\dot{Q}_s$:

$$\eta = \frac{\dot{Q}_c}{\dot{Q}_s} \tag{9}$$

$$\dot{Q}_s = \tau\alpha A_c I_T \tag{10}$$

$$\dot{Q}_c = \dot{m}C_p\left(T_{out} - T_{in}\right) \tag{11}$$

where I_T is the incident solar heat flux density; A_c is the collector surface, τ is the glass's transmission coefficient and the absorption coefficient of the absorber.

3. Boundary Conditions and Numerical Modeling

The boundary conditions used by Abed et al. [5] are adopted in this study, namely uniform temperature and velocity at the collector inlet and atmospheric pressure at the outlet. The study was conducted for a flow rate in the range [20-80 m^3/h], and a constant radiative flux of 850 W/m^2 was applied to the absorber; the lower part of the collector was assumed to be isolated.

The resolution of the system of equations (1)-(4), with imposed boundary conditions, was performed by the finite volume method [18] was used the Fluent commercial code. The Quick second-order scheme (QUICK) was used to discretize the convective terms, and the SIMPLE algorithm [19] is used for the velocity-pressure coupling. The sub-relaxation factors of the solver were used by default to control the update of the calculated variables for each iteration.

4. Mesh Sensitivity Analysis

For a fixed flow rate equal to 80 m^3/h, a refined mesh in the vicinity of the absorber and the isolator was used to capture the strong variations of the temperature and velocity gradients. For this purpose, and to ensure the independence of the mesh on the results, we gradually increased the mesh density as follows: 100×10, 150×20, 200×30, 250×40, 300×50, and 350×60. The results obtained in terms of axial velocity and temperature at the outlet of the manifold show good stability of the grid (250 × 40); for the rest of our simulations, we use the grid just above 300 × 50, which allows us to obtain solutions with a reasonable error.

5. Model Validation and Numerical Results

The experimental data obtained by Labed et al. [5] was adopted to validate the results. The parameters used in their experiments are also listed in Table 1. Figure 4 shows the variation of the temperature at the outlet of the collector as a function of the volume flow rate and confirms a good agreement of our results with those of Labed et al. [5], especially for flow rates higher than 30 m^3/h.

5.1. Thermal approach

The temperature variation at the manifold outlet as a function of flow rate is shown in Fig. 5 for the simple case and different locations, heights, and perpendicular (perp) and inclined (inc) narrowing.

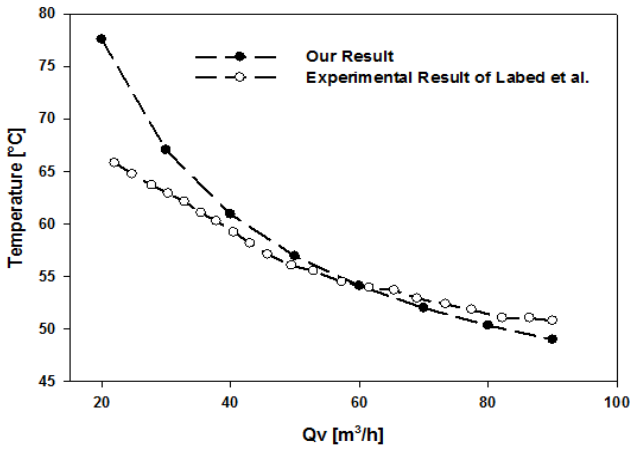

Fig. 4. Temperature at the collector's outlet as a function of the volume flow rate (comparison with Labed et al. [5]).

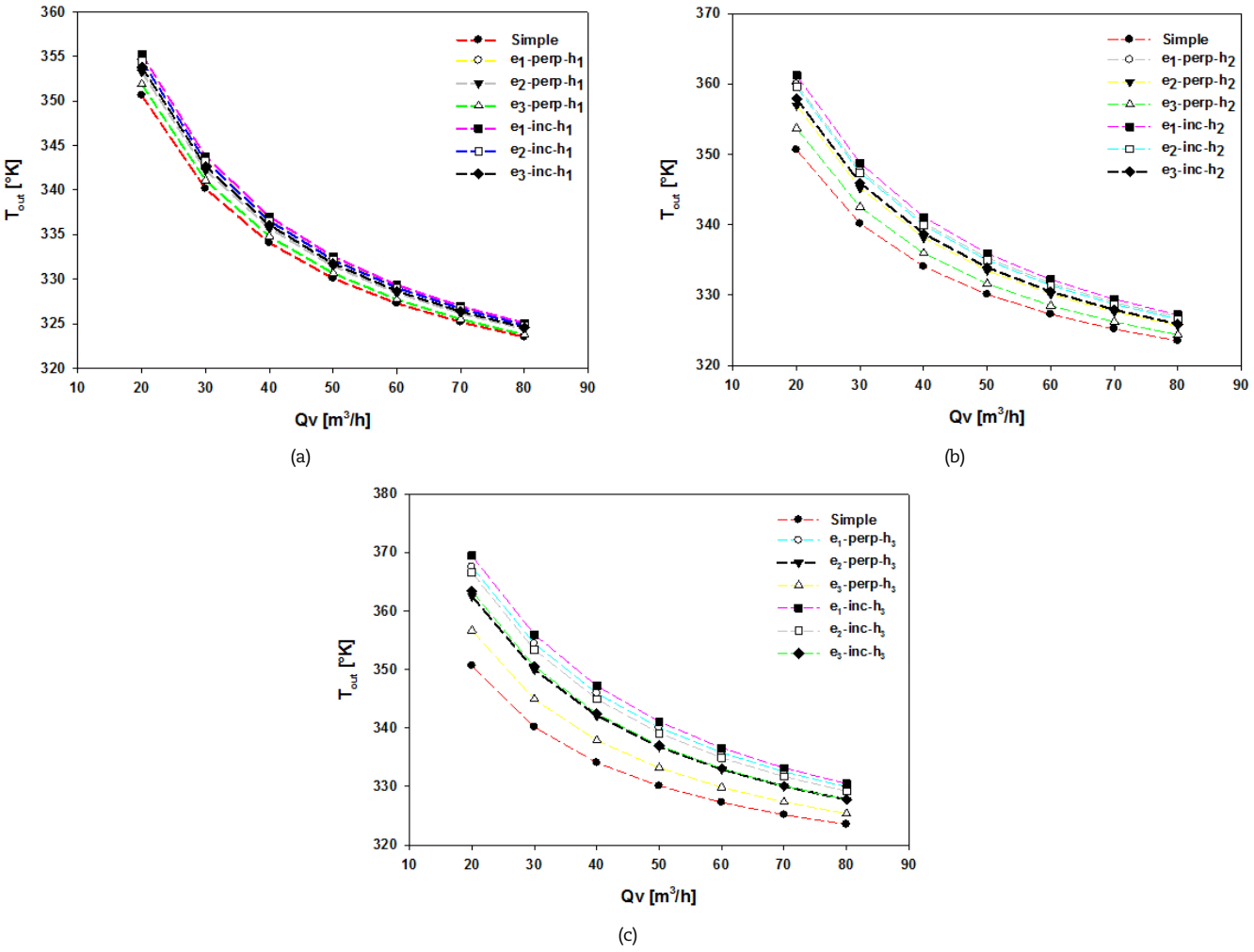

Fig. 5. Variation of outlet temperature with flow rate for different heights: (a) h1, (b) h2, (c) h3.

It can be noted that the increase in airflow is inversely proportional to the outlet temperature. Furthermore, the simple case has the lowest values compared to the other cases. In contrast, the case of an inclined shoulder, for the first position (e1), records the highest temperature values for any height. Table 2 and Fig. 6 show the average inlet-outlet temperature differences calculated over the flow range [20-80] according to the following expression:

$$dT_{aver} = \frac{1}{n}\sum_{i=1}^{n} dT_i \qquad \text{with} \qquad dT = T_{out} + T_{in}$$

where

i	1	2	3	4	5	6	7
Qv [m³/h]	20	30	40	50	60	70	80

Table 2. Calculated average inlet-outlet temperature differences for different heights and positions over the flow range.

	Simple	Perpendicular shoulder			Inclined shoulder		
Height		**e1**	**e2**	**e3**	**e1**	**e2**	**e3**
5	32,98	35,34	34,51	33,62	35,70	35,28	34,83
10		38,68	36,74	34,69	39,40	38,36	37,25
15		43,74	40,29	36,45	44,84	42,82	40,61

Table 3. Absorber exchange surface for perpendicular and inclined shoulders.

	h1			h2			h3		
	e1	**e2**	**e3**	**e1**	**e2**	**e3**	**e1**	**e2**	**e3**
S_{perp} [m²]	1,965	1,965	1,965	1,97	1,97	1,97	1,975	1,975	1,975
S_{inc} [m²]	1,96	1,96	1,96	1,96	1,96	1,96	1,96	1,96	1,96

Table 2 and Fig. 6 confirm that the greater the height or slope of the shoulder, the greater the difference. In addition, an inclined shoulder provides a greater temperature difference (inlet-outlet) than a perpendicular shoulder. This is due to the slope of the shoulder, which helps to eliminate, in a definitive manner, the recirculation zones created by the perpendicular wall of the shoulder (Fig. 7), and therefore ensures greater heat removal at the outlet.

This improvement in heat transfer is independent of the exchange surface since the results in Table 3 confirm that the exchange surface for the perpendicular shoulder case is slightly higher than for the inclined shoulder. Thus, no more influence was observed on this side. It should also be noted that the increase in the relative height at the different locations and thus the increase in the total exchange surface is much more noticeable for the perpendicular case than for the inclined case.

5.2. Dynamic approach

The ratio of the outlet axial velocity, for different perpendicular and inclined shoulders, to the reference velocity as a function of height is shown in Fig. 8.

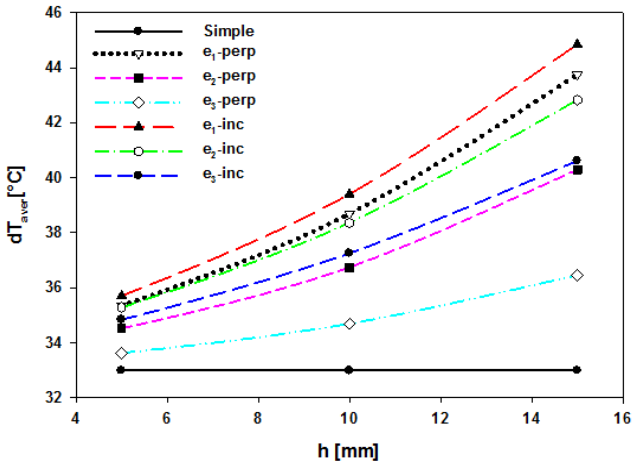

Fig. 6. Average calculated inlet-outlet temperature differences over the flow range for different heights and positions.

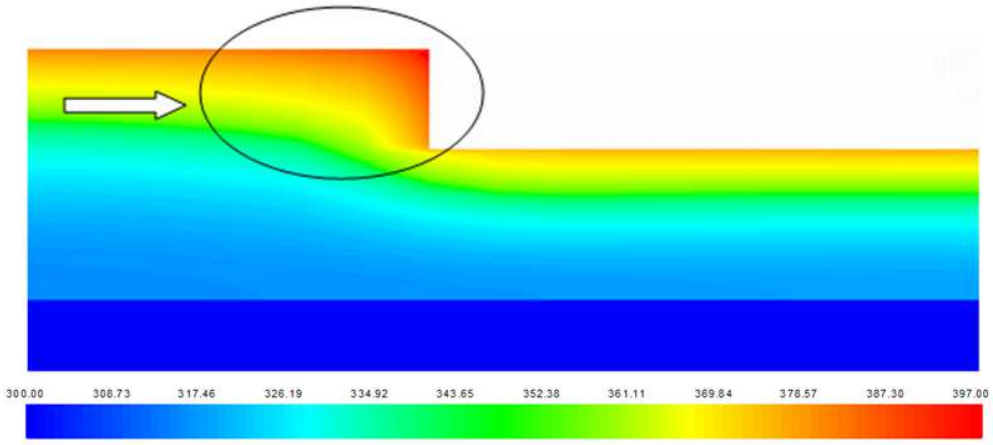

Fig. 7. Temperature contour for a perpendicular shoulder.

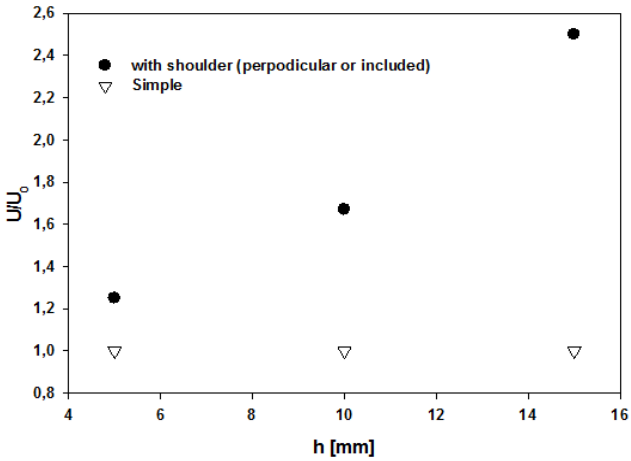

Fig. 8. Ratio of axial velocity-reference as a function of heights.

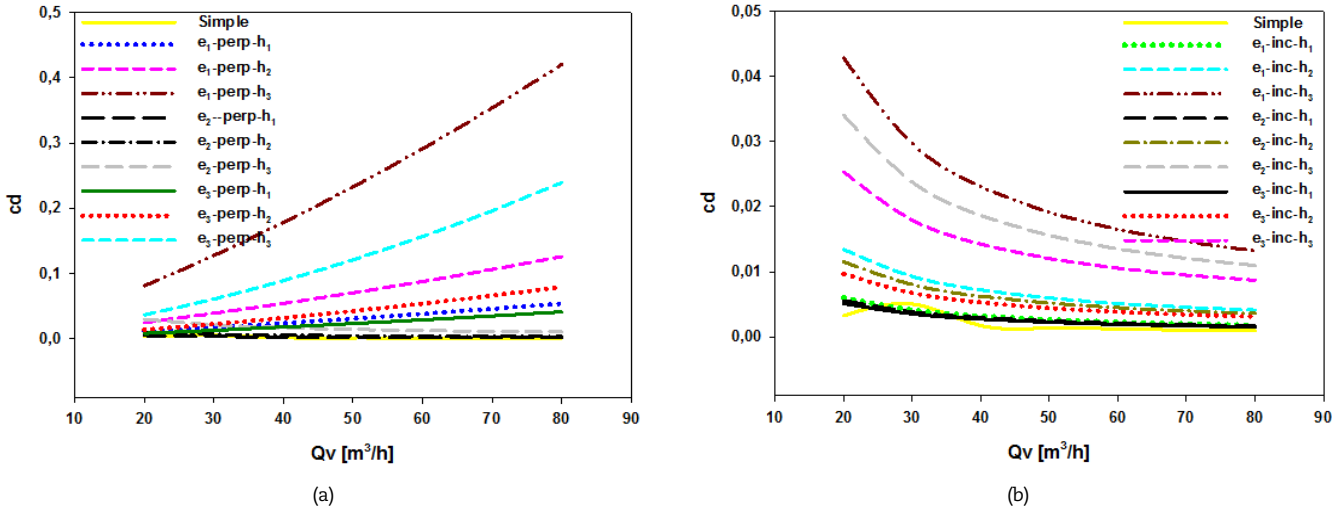

(a) (b)

Fig. 9. Variation of drag coefficient with volume flow rate: (a) sudden narrowing, (b) gradual narrowing.

The results show that the narrowing (sudden or gradual) of the passage section leads to an increase in the ratio of the axial velocity to the reference velocity. This increase is proportional to the height, which records 1.25, 1.67, and 2.50 respectively for heights h1, h2, and h3. Thus, an interest can be mentioned in using a shoulder for applications that require accelerating the flow at the outlet.

Figure 9 shows the evolution of the drag force coefficient for different locations and heights of the shoulder. The case of abrupt narrowing (Fig. 9(a)) shows an increase in Cd with the flow rate Qv, a logical finding since, as Qv and h are increased, the effect of the crash with the corner being perpendicular is increased, subsequently causing more pressure loss and drag. Gradual narrowing (the slope) solves this problem and ensures a decrease in this coefficient by increasing the volumetric flow (Fig. 9(b)) (no accident with an inclined wall). Comparing Fig. 9(a) and Fig. 9(b), it can be seen that either the height or the advancement of the shoulder position directly correlates with the drag. Furthermore, the gradual narrowing solution has drag values of 10% compared to the sudden case.

Figure 10 shows low values of the friction coefficient in the upstream part and a sudden increase (a peak) at the shoulder. Beyond this area, the friction coefficient takes constant and higher values. An analysis of several parameters presented in Fig. 10(a)-(f) for the two types of narrowing, “abrupt and gradual”, is summarized as follows:

- Fig. 10(a) and Fig. 10(b) show that for a fixed location in the middle (e2) and the same height h3, the friction forces decrease with the increasing flow velocity.
- For the same location (e2) and a fixed velocity, Fig. 10(c) and Fig. 10(d) show that the increase in height has a direct effect on the increase in frictional forces.
- For a height h2 and a fixed velocity, Fig. 10(e) and Fig. 10(f) show that the location only affects the position of the peak and not the intensity of the friction, whether it is upstream or downstream of the shoulder.

5.3. Performance analysis

The performance analysis is studied as a function of the variation of the volumetric flow rate (Fig. 11(a) and (b)). It can be seen that the efficiency of the system increases rapidly with the increase of the volumetric flow rate and that the improvements in the thermal performance are recorded for all the cases, compared to the plane collector (simple case).

The efficiency is greater for the inclined shoulder and increases with increasing height, as shown in Fig. 11(a). Table 4 shows that by increasing the height from h1 to h3, the maximum efficiency registers a jump in the order of 8.85% and 8.04% for inclined and perpendicular shoulders, respectively.

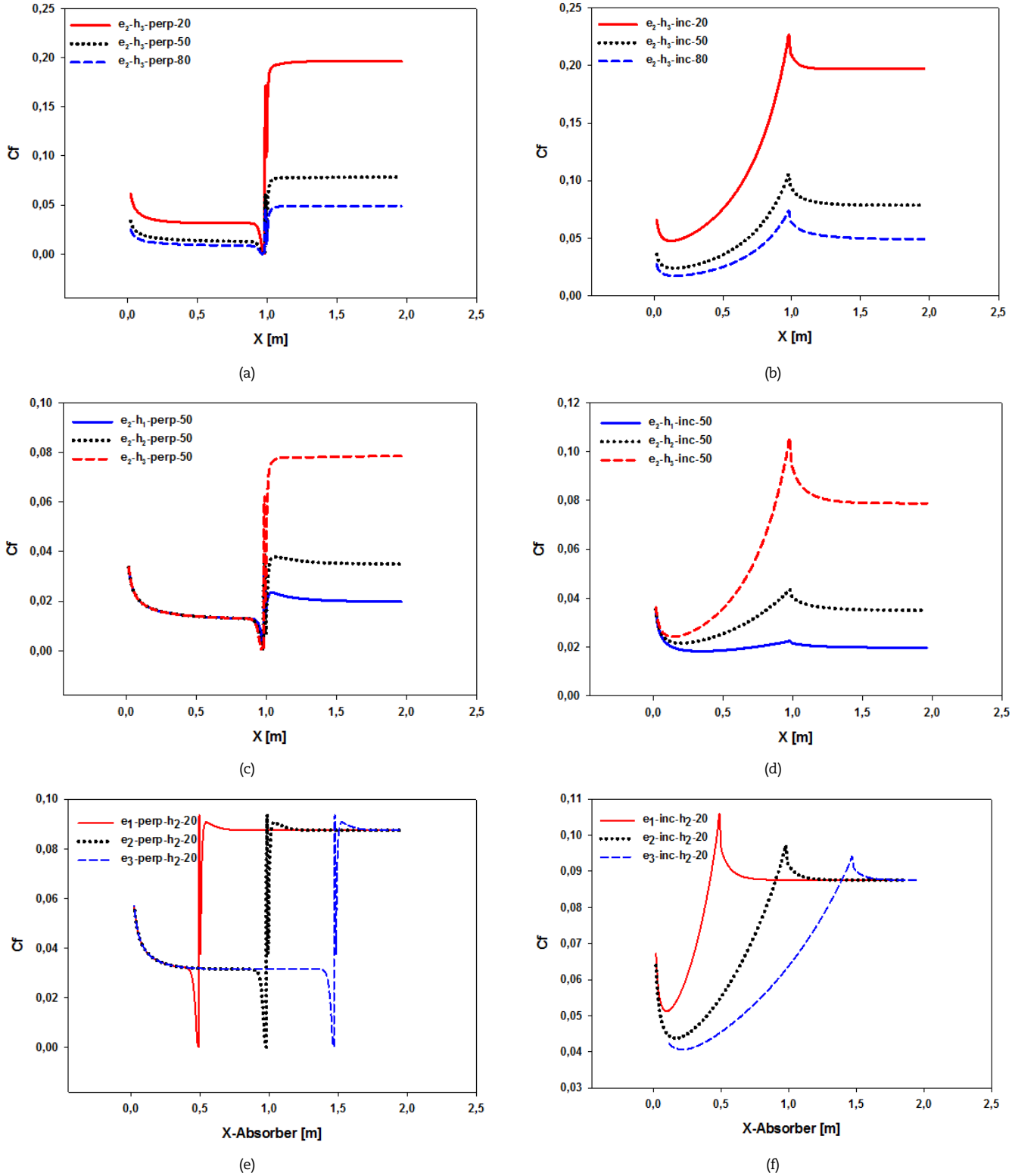

Fig. 10. Friction coefficient along with the absorber for the different cases studied.

Figure 11(b) confirms that the closer the shoulder is positioned to the inlet, the higher the efficiency. The maximum efficiencies obtained, for height h3, for different locations are presented in Table 5 and show significant differences between the shoulders located at L/4 and 3L/4; they are 4.5% for the inclined case and 9.84% for the perpendicular case.

Table 4. Maximum efficiency for the first location e1 and for different heights and types of narrowing.

	h1	h2	h3
$\eta_{max\text{-}inc}$	41.27%	44.75%	50.12%
$\eta_{max\text{-}perp}$	40.82%	43.93%	48.86%
$\eta_{max\text{-}Simple}$		38.66%	

Table 5. Maximum efficiency for different locations and types of narrowing, height h3.

	e1	e2	e3
$\eta_{max\text{-}inc}$	50.12%	47.97%	45.62%
$\eta_{max\text{-}perp}$	48.86%	45.28%	39.02%
$\eta_{max\text{-}Simple}$		38.66%	

Table 6. Comparison between the present study and the results published by various authors for different modifications applied to the absorber of a plate solar collector

Authors	Modification	Mass flow rates /operating parameters	Collector size	Remark
Perwez and Kumar [20] (2019)	Spherical dimple on absorber plate	Experimental analysis 0.009-0.028 kg/s	0.495 m × 1.202 m	23.45-35.50%
Abuska [21] (2018)	Absorber plate with conical surface	Experimental analysis 0.04-0.10 kg/s	1 m × 2 m	57.2-74.6%
Jagannath Reddy et al. [24] (2021)	incorporation of sand of different diameters on the surface of the absorber	Experimental analysis 0,010-0,025 kg/s	2.04 m × 1.04 m	26-42%
Poonam Rani et al. [22] (2022)	The plain absorber plate was modified with the continuous insertion of semicircular loops	Experimental analysis 0,006-0,02 kg/s	-	49.24-76.60% in November 42.26-66.29% in March
Biplab Das et al. [23] (2020)	A sand coated absorber to increase surface roughness and a conventional plain absorber	Experimental analysis 0,01-0,02 kg/s	0.97 m × 0.97 m	19-41%

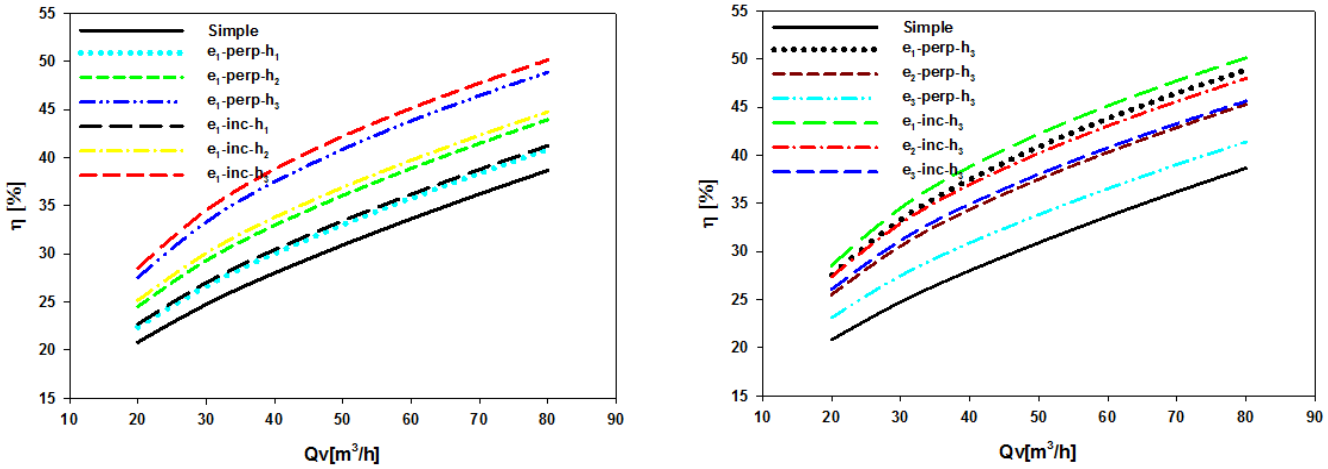

Fig. 11. Variation of collector efficiency with the flow: (a) at different heights, (b) at different locations.

Table 6 shows the comparison between the present study and the results published by various authors for different modifications applied to the absorber in a plate solar collector. Perwez and Kumar [20] determined that the heat transfer rate and instantaneous thermal efficiency of a spherical plate solar air heater are about 1.51 to 1.64 times and 23.45% at 35 and 50%, respectively, higher than a flat plate solar air heater for an air mass flow varying from 0.009 kg/s to 0.028 kg/s.

Abuska [21] compared the thermal performance of an absorber plate with a conical surface and a flat absorber plate in a solar air heater. The average thermal efficiency is obtained in the range 57.2-74.6% for the three mass flow rates of 0.04, 0.08 and 0.10 kg/s. The highest thermal efficiency was determined for the solar air heater with a tapered surface for all operating conditions.

The simple absorber plate in the study by Poonam Rani et al. [22] was modified with the continuous insertion of semi-circular loops. The experiments were conducted at air mass flow rates ranging from 0.006 to 0.02 kg/s. The results indicated that the air mass flow of 0.02 kg/s improved thermal efficiency by 22.03% compared to 0.006 kg/s. In addition, the 0.02 kg/s finned collector gave 19.73-34.3% higher average thermal efficiency than the smooth absorber plate solar collector.

The study by Biplab Das et al. [23] aims to improve the thermal performance of a solar air collector (SAC) by modifying the surface of the absorber and treating two variants of SAC (a sand-coated absorber to increase surface roughness and a conventional ordinary absorber). The results indicated that the SAC with the sand-covered absorber provided additional surface area resulting in increased effective heat transfer. The absolute thermal efficiency of SAC varied from 19% to 41% under the different test conditions.

Jagannath Reddy et al. [24] developed three solar collectors by incorporating sand into the surface of the absorber. Improved energy efficiencies for sand-covered SACs were 26-42% for different air mass flow rates (0.010-0.025 kg/s).

The comparison of the efficiency interval of the solar collector obtained in the present study (Table 4 and Table 5) "38.66-50.12%" agrees with those mentioned in Table 6.

The various modifications proposed in these articles and the review by Elumalai and Ramalingam [15] and Chinmaya Mund et al. [17] have brought a marked improvement in the performance of the collector but also an increase in the pressure drop. On the other hand, the present study shows an effective solution to improve the system by decreasing friction and drag. The drag values in the case of gradual narrowing are 10% compared to the sudden case.

The published articles have not improved the dynamic aspect, whereas this paper reveals that the sudden or progressive narrowing of the passage section increases the ratio of the "input-output" axial velocity from 1.25 to 2.50. Therefore, it can be a useful solution for applications requiring faster output flow, such as drying.

6. Conclusion

This study evaluated the performance of an air-cooled solar collector in the presence of a narrowing system. Two narrowing patterns were studied, the first is steep using a perpendicular wall shoulder, and the second is gradual with an inclined slope. Three shoulder locations, each with three different heights, were also analyzed and compared to the simple case. The results indicate the presence of a constriction in the air stream of a flat plate solar collector remains an effective way to improve its dynamic and thermal performance.

- The fluid velocity can reach proportions ranging from 1.25 to 2.50 times the reference velocity depending on the case studied.
- The pressure losses are of the order of a few tenths in the case of an inclined shoulder compared to the perpendicular case.
- An angled shoulder appears to be an innovative solution that eliminates the dead zone, significantly reduces friction and drag forces, and reasonably improves heat transfer in the system.
- Gradual narrowing maximizes heat transfer at a low cost (without increasing the exchange surface) and the least possible losses.
- The study of the system's efficiency showed a slight advantage for the inclined shoulder case (50.12% with h3) compared to the perpendicular case (48.86%); the simple case with an efficiency of 38.66% is well below both cases.
- According to the cases studied, an increase in height can ensure a gain in efficiency of around 8.85% for the inclined case and 8.04% for the perpendicular case.
- Finally, advancing the shoulder position (from e3 to e1) can also provide a positive difference in the efficiency of about 4.5% for the inclined case and 9.84% for the perpendicular case.

Author Contributions

H. BENZENINE conducted the numerical simulations; S. ABBOUDI developed the cases studied with mathematical modelling. The manuscript was written with the contribution of all authors. All authors discussed the results, reviewed and approved the final version of the manuscript.

Acknowledgments

Not applicable.

Conflict of Interest

The authors declared no potential conflicts of interest with respect to the research, authorship and publication of this article.

Funding

The authors received no financial support for the research, authorship and publication of this article.

Data Availability Statements

The datasets generated and/or analyzed during the current study are available from the corresponding author on reasonable request

Nomenclature

A_f	Fluid flow cross-section, m^2
A_0	Wetted surface, m^2
C_d	Drag coefficient
$\overline{C}_f$	Average friction coefficient
C_p	Specific heat, J/(kg.°C)
G	Height between the transparent cover and the absorbing plate, m
H	Height of the shoulder, m
H	Height between the absorber and the lower plate, m
I	Height of the insulation , m
L	Channel length, m
l	Channel width, m
P	Pressure, Pa
T	Temperature, C
U_{in}	Inlet velocity, m/s
$\overline{U}$	Mean velocity in channel, m/s
u, v	Axial, vertical velocity, m/s
x, y	Axial, vertical directions, m

Greek Letters

ρ	Density, kg/m^3
K	Thermal conductivity, W/(m.°C)
μ_f	Dynamic viscosity of fluid, kg/(m.s)
ν	Kinematic viscosity, m^2/s
τ_w	Shear stress to the wall, $kg/(m.s^2)$
Δp	Pressure losses, Pa

Subscripts and Superscripts

in, out	inlet, outlet of the test section
W	Wall
f	Fluid
S	Solid
i, j	Refers coordinate direction vectors

Abbreviation

Inc	Inclined
Perp	Perpendicular
ei	Position of the shoulder, i=1,2,3

References

[1] Rahman, M.M., Saha, S., Mojumder, S., Naim, A.G., Saidur, R., Ibrahim, T.A., Effect of Sine-Squared Thermal Boundary Condition on Augmentation of Heat Transfer in a Triangular Solar Collector Filled with Different Nanofluids, *Numerical Heat Transfer, Part B: Fundamentals*, 68(1), 2015, 53–74 .
[2] Yang, Y. T., Chen, P. J., Numerical Study of a Solar Collector with Partitions, *Numerical Heat Transfer, Part A: Applications*, 66(7), 2014, 773–791.

[3] Nasrin, R., Parvin, S., Alim, M.A., Heat Transfer and Collector Efficiency through a Direct Absorption Solar Collector with Radiative Heat Flux Effect, *Numerical Heat Transfer, Part A: Applications*, 68(8), 2015, 887–907.
[4] Said, Z., Sajid, M.H., Saidur, R., Mahdiraji, G.A., Rahim, N.A., Evaluating the Optical Properties of TiO2Nanofluid for a Direct Absorption Solar Collector, *Numerical Heat Transfer, Part A: Applications*, 67(9), 2015, 1010–1027.
[5] Labed, A., Moummi, N., Aouès, K., Zelloufand, M., Moummi, A., Etude théorique et expérimentale des performances d'un capteur solaire plan à air muni d'une nouvelle forme de rugosité artificielle, *Revue des Energies Renouvelables*, 12(4), 2009, 551–561.
[6] Abene, A., Dubois, V., Le Ray, M., Ouagued, A., Study of a solar air flat plate collector: use of obstacles and application for the drying of grape, *Journal of Food Engineering*, 65, 2004, 15–22.
[7] Ahmed-Zaïd, A., Moulla, A., Hantalaand, M.S., Desmons, J.Y., Amélioration des Performances des Capteurs Solaires Plans à Air: Application au Séchage de l'Oignon Jaune et du Hareng, *Revue des Energies Renouvelables*, 4, 2001, 69-78.
[08] Gopi, R., Ponnusamy, P., Fantin Arokiaraj, A., et al., Performance comparison of flat plate collectors in solar air heater by theoretical and computational method, *Materials Today: Proceedings*, 39, 2021, 823-826.
[9] Mzad, H., Prediction of thermal performance of double-glazed solar collector, *Archives of Thermodynamics*, 29(1), 2008, 71–86.
[10] Mzad, H., Otmani, A., Haouam, A., Lopata, S., Oclon, P., Tilt optimization of a double-glazed air solar collector prototype, *MATEC Web Conf.*, 240, 2018, 0400.
[11] Ravi, R.K., Saini, R.P., Nusselt number and friction factor correlations for forced convective type counter flow solar air heater having discrete multi V shaped and staggered rib roughness on both sides of the absorber plate, *Applied Thermal Engineering*, 129, 2018, 735-746.
[12] Ahmad, M.J., Tiwari, G.N., Optimization of tilt angle for solar collector to receive maximum radiation, *The Open Renewable Energy Journal*, 2, 2009, 19–24.
[13] Yang, M., Wang, P.S., Yang, X.D., Shan, M., Experimental analysis on thermal performance of a solar air collector with a single pass, *Building and Environment*, 56, 2012, 361–369.
[14] Ravi, R.K., Saini, R.P., Experimental investigation on performance of a double pass artificial roughened solar air heater duct having roughness elements of the combination of discrete multi V shaped and staggered ribs, *Energy*, 116, 2016, 507–516.
[15] Elumalai, V., Ramalingam, S., A review on recent developments in thermal performance enhancement methods of flat plate solar air collector, *Renewable and Sustainable Energy Reviews*, 134, 2020, 110315.
[16] Benli, H., Determination of thermal performance calculation of two different type solar air collectors with the use of artificial neural networks, *International Journal of Heat and Mass Transfer*, 60, 2013, 1–7.
[17] Chinmaya, M., Sushil, K.R., Ranjit, K.S., A review of solar air collectors about various modifications for performance enhancement, *Solar Energy*, 228, 2021, 140-167.
[18] Patankar, S.V., *Numerical Heat Transfer and Fluid Flow*, Hemisphere, New York, USA, 1980.
[19] Patankar, S.V., Spalding, D.B., A calculation procedure for heat, mass and momentum transfer in three-dimensional parabolic flows, *International Journal of Heat and Mass Transfer*, 15, 1972, 1787-1806.
[20] Perwez, A., Kumar, R., Thermal performance investigation of the flat and spherical dimple absorber plate solar air heaters, *Solar Energy*, 193, 2019, 309–323.
[21] Abuska, M., Energy and exergy analysis of solar air heater having new design absorber plate with conical surface, *Applied Thermal Engineering*, 131, 2018, 115–124.
[22] Poonam, R., Tripathy, P.P., Experimental investigation on heat transfer performance of solar collector with baffles and semicircular loops fins under varied air mass flow rates, *International Journal of Thermal Sciences*, 178, 2022, 107597.
[23] Biplab, D., Jayanta D.M., Suman, D., Zacharopoulos, A., Effect of the absorber surface roughness on the performance of a solar air collector: An experimental investigation, *Renewable Energy*, 152, 2020, 567-578.
[24] Reddy, J., Roy, S., Das, B., Jagadish, Performance evaluation of sand coated absorber based solar air collector, *Journal of Building Engineering*, 44, 2021, 102973.

ORCID iD

Hamidou Benzenine https://orcid.org/0000-0002-7932-5267
Said Abboudi https://orcid.org/0000-0001-7420-1014

How to cite this article: Benzenine H., Abboudi S. Impact of the Narrowing System at Different Locations and Heights on the Performance of a Plane Solar Collector, *J. Appl. Comput. Mech.*, 8(4), 2022, 1445–1455.
https://doi.org/10.22055/jacm.2022.39487.3414